V-SPARS: A COMBINED SAIL AND RIG SHAPE RECOGNITION SYSTEM USING IMAGING TECHNIQUES

D.J. Le Pelley[1], d.lepelley@auckland.ac.nz
O. Modral[2], o.modral@auckland.ac.nz

Abstract. Measurement of flying sail shapes is an extremely useful technique both for design and for use whilst racing. Until now, no simple method of measuring highly curved downwind sails has been found. In this paper, a method called Visual Sail Position And Rig Shape (V-SPARS) is presented which addresses this issue. The system uses deck mounted cameras to look up at stripes marked on the sails and has the ability to correct for large perspective effects. In addition, the rig deflection is measured from the displacement of target points and is combined with the sail shapes to give a global position of the sails and rig above the deck. This paper despresents a validation of the system for many different types of sails and, through the results of wind tunnel experimentation, shows a number of ways in which the system can be used. Conventional upwind sail testing has been carried out in a wind tunnel using V-SPARS to accurately measure the sail stripes and simultaneous rig position. The system has been used with downwind sails to capture the highly curved shapes and global locations of a gennaker flying from a bowsprit.

NOMENCLATURE

α	Horizontal angle of point on stripe from camera to centre line
AWA	Apparent wind angle
β	Vertical angle of point on stripe from camera to centre line
C_L	Lift coefficient
C_D	Drag coefficient
$\Delta x, \Delta y$	Camera calibration parameters
dX, dY	Flying luff offset values
γ	Angle of sail to the vertical at stripe luff
θ	Stripe chord angle to centre line

1. INTRODUCTION

Measurement of sail flying shape is performed for many reasons. It is still not easy to predict the sail flying shape accurately at the design stage and full-scale measurements can be used to validate this and enable further design optimisation. Capture of sail shape enables accurate numerical simulations in CFD, and enables validation of sail elasticity and finite element codes. One of the most important reasons to know the sail shape is for creation of a sail database that can be linked with performance data, and the ability to trim to known targets in real-time.

The majority of sail vision systems [1,2] incorporate cameras at the head of the mast and forestay looking down at stripes on the sail. These systems work well for upwind sailing conditions and only employ simple correction algorithms for perspective as the sail stripes tend to stay relatively orthogonal to the camera. Some research systems also incorporate pictures taken looking upwards to determine more information about the head of the sails [3] and to give true 3D photogrammetry. [4]. These types of system cannot be used for looking at offwind sails. One of the main disadvantages is the amount of weight and windage required aloft for such a system. Some of these systems have been used to measure masthead twist to some extent by noting perceived movement of deck targets under load.

Recently, advances have been made with laser scanning technology for capturing the highly curved downwind sail shapes, both in the wind tunnel [5] and at full scale. The measurement accuracy of such systems is extremely good, although the disadvantage with this system is that it takes a significant period of time to scan the sail during which the sail moves about.

In the controlled environment of the wind tunnel, many systems are used to capture both upwind and downwind sail shapes [6,7]. Most of these make use of stereo-photography techniques where the sail is captured by multiple cameras from off the boat. The accuracy of these systems can be high. Similar systems have also been used at full scale using single cameras from multiple locations [8]. The accuracy of such systems is unknown and both types of system rely on external support, preventing use whilst racing.

The aim of this project was to develop a simple system using a single camera on the boat for each sail. The cameras are mounted in the deck looking up, and are able to cope with large perspective effects and stripes with very high curvature. The result is V-SPARS (*Visual Sail Position And Rig Shape*): a system using inexpensive off-the-shelf digital cameras which combines the headsail, mainsail and rig positions to give their full 3D global position above the deck.

---

[1] Wind tunnel manager, Yacht Research Unit, University of Auckland
[2] Wind tunnel engineer, Yacht Research Unit, University of Auckland

2. V-SPARS

2.1. Overview

V-SPARS uses cameras mounted at deck level looking upwards at the sails and rig. The aim of the system is to determine the global location in Cartesian coordinates of specific targets on the sails and rig. For the rig, these targets comprise coloured dots which are placed at different heights on the mast, typically under the spreaders or at diagonal crosses. On the sails, coloured horizontal stripes are applied to the mainsail, jib and downwind sails. The system is able to dynamically track the stripes, calculate the stripe coordinates in 3D space and link the stripe position to the rig deflection. This enables not only the conventional trim changes to be seen, but also rig tuning can be carried out using this system, a job which until now has only been carried out by eye.

Figure 1. V-SPARS giving real-time downwind flying sail shapes in the wind tunnel (camera location indicated)

The main advantage of V-SPARS over other visualisation systems is that it is able to deal with large perspective effects. Even systems that look up or down at the stripes from the centre of the chord can still have significant perspective effects at the luff and leech of the stripes. By accounting for these effects, it is possible to place a camera in the optimum position to see as much of the sail as possible whilst still producing an accurate sail shape. This also enables the system to cope with large changes in sheeting angle. This has been shown to work even for the highly curved stripes in offwind sails. A typical screenshot of the software operating in the wind tunnel can be seen in Figure 1, where the location of the camera on the model, at the end of the bowsprit in this case, is indicated by the white arrow.

The main steps of the software can be seen in Figure 2. The program essentially takes images using the required camera(s), automatically finds the sail stripes and rig targets, and then combines the results of all the data to give the global X, Y and Z coordinates of the sail stripes and rig relative to the boat origin.
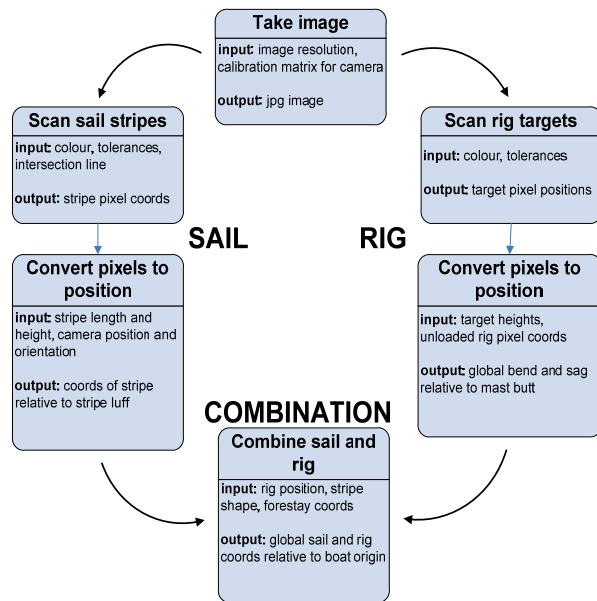

Figure 2. Flow chart of V-SPARS

2.2. Camera calibration

Initially, each camera needs to be calibrated to enable the barrelling and distortion effects of the lens to be removed. At this stage it is not necessary to correct for perspective effects as this will be done later in the process. A simplified procedure based on [9] was used. A single image of a checkerboard is taken carefully at a known distance from the surface. The known position of the squares as seen by a pinhole camera with no distortion, but which includes perspective effects, can be calculated. This is compared with the actual digitised square position. Then 3D interpolated surfaces of pixel position error (Δx, Δy) can be produced for the entire field of view, In the subsequent analysis, all image coordinates are corrected using these surfaces before further calculation.

2.3. Sail stripe recognition

For a chosen image, the two main user inputs required are a stripe colour and a graphically picked straight line through which all the sail stripes pass. A number of passes along this line are then made, assessing the colour of each pixel and seeing if it is a match within user-defined tolerances. These possible points are categorised into possible stripes based on their proximity to each other and their relative gradients. Once the stripe has been identified, it is traversed to determine its bounds by sweeping perpendicular to the gradient of the points found so far. Adjustment of expected stripe width and expected colour allows an optimisation of this routine. The output is a list of pixel coordinates defining the top edge of each stripe.

2.4. Rig target recognition

Initially, the rig target positions are acquired manually. The user clicks anywhere within each coloured target dot on the rig and the program automatically finds the centroid of all surrounding pixels within the colour tolerance. This enables sub-pixel accuracy and, at full scale, results in a resolution of better than 5mm at the top of a 30m rig using a 5 mega-pixel camera. For subsequent passes, the program searches for each dot in an area around its previously recorded position and, once found, the centroid is computed in a similar manner and stored as the new location.

2.5. Converting to real-world coordinates

Figure 3 shows a diagram of the key parameters for an example of determining the shape of a typical downwind sail stripe, and will be referred to in the explanation below.
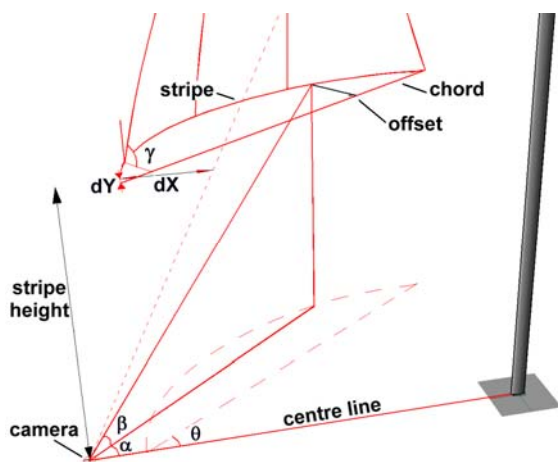

Figure 3. Diagram showing key parameters for stripe shape determination

During the setup process, a photograph is manually digitised to determine the "zero" luff position of each stripe. For the mainsail, this is the stripe luff position on the unloaded mast. For the jib and downwind sails, this is a photographed tight string line or halyard with markers attached at the different stripe heights, and is indicated by the dotted line in Figure 3. By knowing the locations of the ends of the string and the height of each marker, the flying sail luff position (or forestay sag in the case of a jib) forestay sag can be determined. This is done by measuring the change in luff position of the flying sail, indicated by dX and dY in Figure 3.

The stripe chord angle to the boat centre line (θ) is calculated from the detected locations of the luff and leech of the stripe and by taking into account the camera orientation to the centre line of the boat.

Once the global position of the luff of each stripe is known, the distance from the camera to the luff can easily be calculated.

At this stage, a guess has to be made about the length of the chord line joining the luff and leech by assuming it is a certain percentage of the stripe length. Eventually the whole calculation is iterated as many times as is necessary to minimise this assumption. By estimating this, in combination with the angle θ and the height above deck, the distance from the camera to the leech can be calculated. This allows the chord line to be defined in 3D space along which all the perpendicular offsets will be located.

The following few operations take place as they would if there were no perspective effect at all, and in image coordinates. The distance around the curve in pixels from the luff to each digitised point is first found, assuming a linear distribution at this stage. Then the point on the chord line normal to each curve point is determined. The distance between these two points is an uncorrected offset distance in pixels.

The next stage is to correct for the perspective effects. Firstly, the distance of each point on the curve from the camera is estimated from the previously calculated leech and luff distances. This distance and the horizontal and vertical angles (α and β respectively), shown in Figure 3, are then used to calculate two stretch factors:

- a factor to stretch the length of the offset segment
- a factor to slide this offset segment along the chord line.

These stretch factors are applied to the offset line and the position of this line along the chord respectively, for each point on the stripe. Camera calibration parameters are used in this process to convert from pixels to real-world coordinates.

Now the vertical angle of the camera to the stripe (γ) is found by comparing the visible stripe width at the luff in the picture to the known physical stripe width on the sail. The stripe offsets calculated above are divided by the cosine of this angle to give the final stripe depths.

At this stage, the initial estimate of the chord length can be improved. The known curve length is numerically "draped" over the offsets positioned along the chord line. The chord is stretched such that the curve length exactly fits the offsets. The whole process is then iterated until there is no significant change in the calculated chord length.

This stripe shape and angle are then applied to the initially calculated luff position and the result is a set of Cartesian coordinates of the stripe relative to the yacht's origin.

The program is able to cope with the camera being positioned outside the boundary of the sail (ie. forward of the tack) so that theoretically any camera position that can see all of the stripes can be used. Only a small range of camera positions has so far been examined The camera should ideally be positioned as centrally as possible to minimise the perspective effects.

For the case of the rig, the deflection is calculated relative to a previously taken picture with the mast unloaded. Even in this case, the jack-up load on the rig will usually make the mast tube assume a curved shape, so a theodolite or plumb line is used to measure the initial offset at each height at the time this picture is taken. The loaded rig deflection is then calculated by finding the X and Y deflection in pixels between the loaded and unloaded pictures, and then converting these into real-world distances by knowing the distance of each target from the camera and the camera calibration properties. The twist relative to the dock picture is also found at heights where two targets can be used, such as the underside of spreaders. A perspective adjustment is made in a similar way to the sail stripes to account for the camera not being positioned directly beneath the targets.

Combining the data for all sails and the mast results in a global point cloud defining the sail and mast locations in 3D space. These can be plotted visually, added to a database, used to reconstruct the sail for CFD calculations, etc. With the current system, nothing is known about the foot of the sail below the bottom stripe, although it is hoped that the use of a wide angle lens will allow this information to be captured.

The main assumption used to convert the image coordinates to real-world locations is that the stripes are in the horizontal plane when flying, which simply requires stripes that are not necessarily aligned with the broadseams. This can be easily predicted at the design stage. Typically, for a downwind sail with a stripe which is at an angle of 10° to the horizontal, and having a maximum depth equal to 10% of the chord length, the error is about 0.4% of the chord length, or 4% of the maximum stripe depth. The flying height of the downwind sail tack above the deck or sprit also needs to

be estimated in advance and allowed for in all of the calculations, although its effect is usually small.

2.6. Hardware and wind tunnel setup

The mainsail requires one camera for each tack, mounted nominally at ½ beam off the centreline just aft of the spreaders. The jib and downwind sail cameras are mounted wherever the full stripes can be best seen. In this study with conventional lenses, it was necessary to mount the jib camera at the forestay and the downwind camera at the end of the sprit. With wide angle lenses it should be possible to mount the cameras closer to the centre of the stripes which should improve accuracy. These will also allow a single camera for each sail to be used for both tacks, which is the overall aim of the system. The mainsail requires two separate cameras because of the interference of the boom and the requirement to be off centreline. A schematic of the wind tunnel setup and camera locations used in the following research is shown in Figure 4.

2.7. Application to full scale

The testing detailed in this paper has all been carried out in The University of Auckland's Twisted Flow Wind Tunnel [10]. V-SPARS has been designed for use on the water and that is the next stage of development. All of the techniques that have been developed here can be used at full-scale. The biggest issue is the changing background colour of the image and effects of sun on the camera. These effects can be mitigated to some extent with careful positioning and imaging techniques, and the rig positioning part of the system has been shown to work well at full scale with previous unpublished work on IACC yachts. However, this remains the biggest drawback with look-up systems.
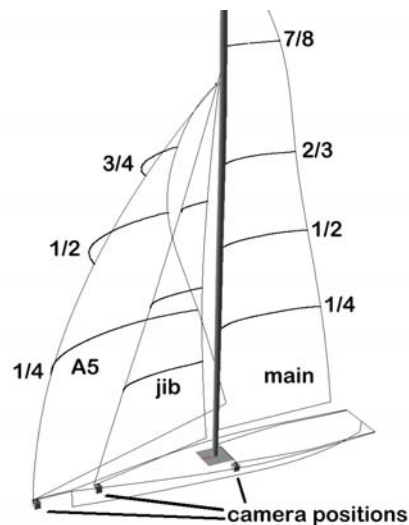

Figure 4. Schematic of camera positions and sails tested

3. VALIDATION

3.1. Overview

The majority of the validation cases presented here were carried out with the software still in development. The pictures were manually digitized and the stripe data calculated in a spreadsheet using the same algorithms. This meant that fewer points along the stripe were used than in the software, where typically the software analyses a point at every 10th pixel which allows the wrinkles and local data to be captured with the stripe.

3.2. Solid mainsail

The first set of validation measurements were carried out on the generic wind tunnel model using a solid fiberglass mainsail so that the shape could be easily measured in advance. These initial tests looked at a range of boom positions between centerline and about 60 degrees off centerline. The main focus in all of these tests was the bottom stripe as the perspective effect is the most significant here. Figure 5 and Figure 6 show the stripe and results respectively for a typical case. The agreement is within 2mm.

Figure 5. V-SPARS photograph of solid mainsail for bottom stripe validation
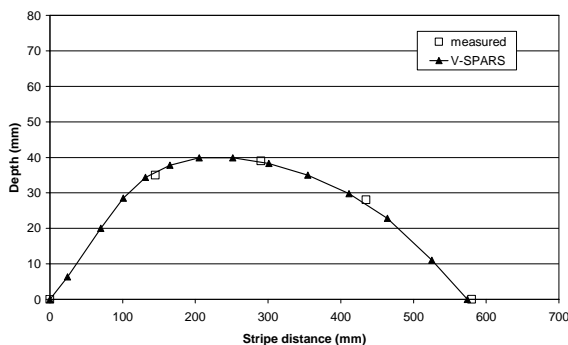
Figure 6. V-SPARS v. known depth of solid mainsail bottom stripe

3.3. Solid spinnakers

In order to test the ability of V-SPARS to deal with some highly curved surfaces, a solid spinnaker model [11] was used. Figure 7 shows the photo and Figure 8 shows the resulting stripe depth measured by the software. The

agreement shown here is good, but this is not always the case for these highly curved surfaces. This situation represents the limits of what the perspective correction model can accurately achieve. Also, there is currently no way of knowing the luff position in global coordinates when the sail is flown from a spinnaker pole instead of a fixed bowsprit. This, however, is not seen as a limitation for the intended applications, which are generally asymmetric sails flown from the bowsprit.

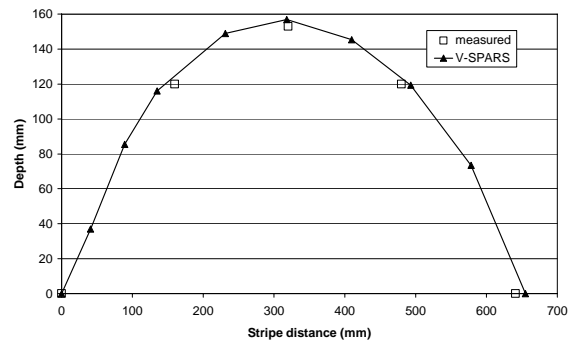Figure 7. V-SPARS photograph of solid spinnaker for stripe validation

Figure 8. V-SPARS v. known depth of solid spinnaker bottom stripe

3.4. Soft jib and A5

The remaining validation cases were carried out in a similar manner to conventional sail testing, with the soft sails flying in the wind tunnel. The main difficulty with this is related to the ability to measure accurately the actual sail shape for validation without getting too close to the model and thereby changing the pressure field. A system was developed with an array of contact sensors that can be remotely positioned on the leeward side of each stripe. Even with this system, the achievable accuracy was only about +/- 2mm.

Figure 9 shows the jib at 30º apparent wind angle (AWA) and Figure 10 presents the resulting V-SPARS shapes compared with the measured shapes for all 3 stripes.
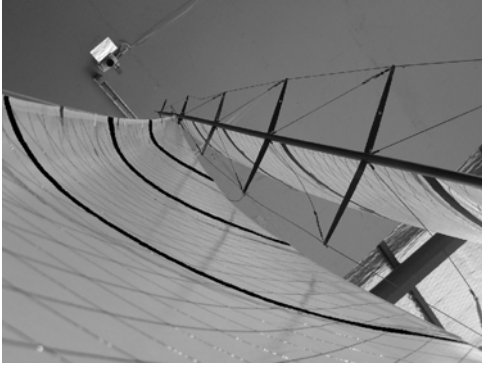
Figure 9. V-SPARS photograph of soft jib for stripe validation
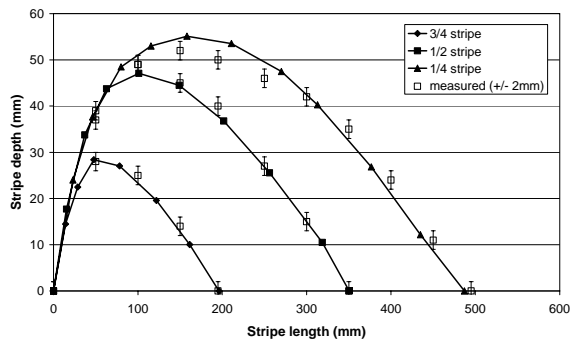

Figure 10. V-SPARS v. known depth of soft jib

Arguably the most important test case is for a deep flying sail. In this case it was not possible to use the contact sensor system and it was necessary to revert to string and a ruler, which reduces the accuracy to +/- 5mm. A better measurement technique would be preferable for this validation. Figure 11 shows the sail photo and Figure 12 gives the result of the validation.
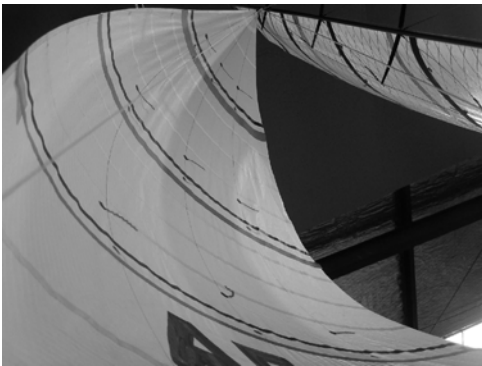

Figure 11. V-SPARS photograph of flying A5 at 60º AWA for stripe validation
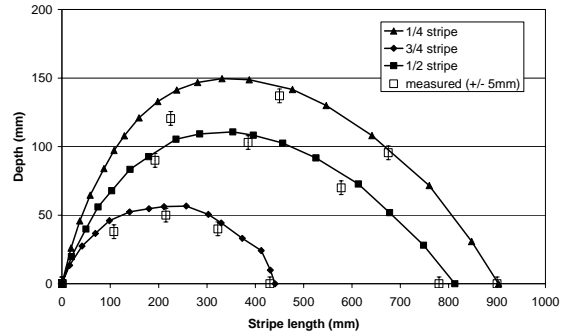
Figure 12. V-SPARS v. known depth of flying A5 at 60º AWA

3.5. Summary of validation

It can be seen from the previous cases that the accuracy of the system is dependent on the type of sail being flown. For these cases, the front camera was mounted at the forestay and on the end of the bowsprit for the jib and A5 respectively. This was necessary in order to capture the full stripes as low as possible on each sail, but results in some very large perspective effects which reduce the accuracy of the stripe shape estimation. A wide-angle lens would allow a camera mounted in the centre of the foredeck to be closer to the centre of each stripe. This should improve the accuracy of the shape estimation and also would allow a single camera to capture both jib and downwind sail stripes on both tacks without repositioning.

The top stripe of the A5 is also very difficult to predict because the vertical angle of the head rotates the stripe normal relative to the camera. In this case the known stripe width at the luff is used to estimate the vertical angle in the calculation process, but large vertical angles seem to lead to significant errors.

From all of the validation studies, including many not presented here on various static curved shapes, the depth accuracy can be summarized as:
- Mainsail: error <0.5% stripe length
- Jib: error < 1% stripe length
- Downwind sail: <2% stripe length

In most cases the downwind sail was predicted much better than 2% but this value covers all outlying cases tested. These values include all possible sheeting angles for these sail types.

Generally the maximum draft position was well predicted. The errors in both depth and position appear to remain consistent for similar types of sails and camera positions, allowing accurate comparative tests between different sails.

4. V-SPARS USED IN WIND TUNNEL STUDIES

4.1. Upwind sweeps

Typical upwind testing was conducted in The University of Auckland's Twisted Flow Wind Tunnel [12] on an America's Cup 90' Class (AC90) model with a conventional mainsail and "jib". The jib model was actually a relatively deep draft reaching sail with a significant luff curve from another yacht type, to enable sensible sail shapes at deeper wind angles. V-SPARS was used with a camera mounted just aft of the shrouds for the mainsail and rig, and a camera mounted in the foredeck near the forestay for the jib position. The tests below were performed at a fixed heel angle and comprised a trim sweep from over-sheeted to under-sheeted for apparent wind angles of 20º, 25º and 35º. The wind angles were deliberately deep for this study, compared with typical AC90 upwind apparent wind angles of around 17º. This was to demonstrate the ability of V-SPARS to predict the eased sail shapes. The purpose of the results presented in this section is to demonstrate ways in which V-SPARS can augment conventional sail testing in the wind tunnel.

Figure 13 shows the lift and drag coefficients (C_L and C_D) for the tested apparent wind angles.
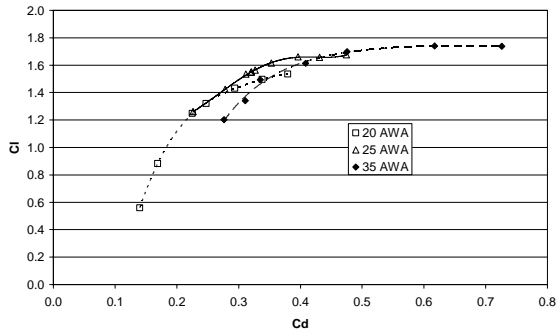

Figure 13. Lift versus drag coefficient for mainsail and jib combination

It is possible to use the *power* parameter to look at the trim trends [13]. The *power* parameter is defined as the rolling moment for each case divided by the rolling moment for the optimum trim (in this case the highest C_L/C_D value). For 35º AWA, Figure 14 shows a plot of the mainsail and jib draft values against *power* and Figure 15 shows the twist angles, defined as the horizontal angle of the stripe chord from centerline, plotted against *power*. It is interesting to note the similarity in behaviour of jib and mainsail stripes at similar heights. It should be noted that the heel angle was fixed and did not change for different values of *power*.
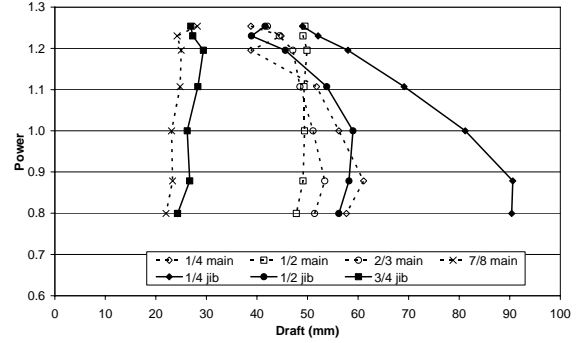

Figure 14. Variation of *power* with draft of main and jib at 35º AWA
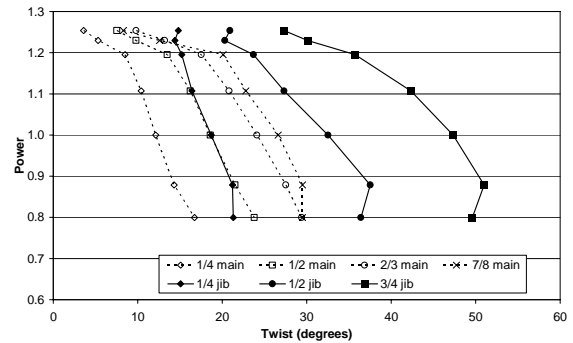
Figure 15. Variation of *power* with twist of main and jib at 35º AWA

In Figure 16, the mainsail and jib stripes at similar heights have been averaged and combined (the mainsail 7/8 stripe has been omitted for the 20º AWA case) to give some idea of how the sails work in combination. The large dot marks the tightest trim and the line then shows the path of successive easing. The twist angles (solid lines) are the horizontal angle of the stripe from centerline. A clear optimum twist angle for each stripe-pair can be seen. The dotted lines represent the maximum draft of the stripe-pair. For the bottom stripe the draft increases with ease whereas for the top stripe (3/4 jib paired with 2/3 mainsail) the draft decreases as the leech tension is eased.
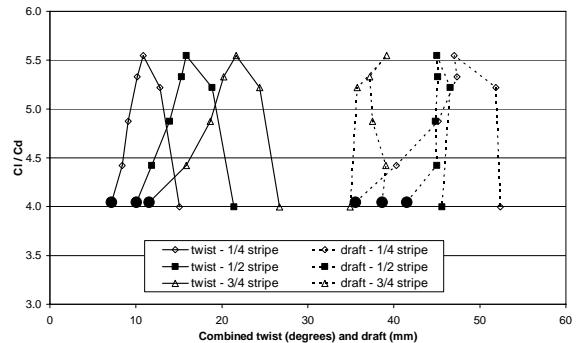
Figure 16. Variation of C_L/C_D with twist and draft of combined mainsail and jib stripes at 20º AWA

4.2. Rig position

One of the main advantages of V-SPARS over other vision systems is the ability to look at rig tune in combination with sail trim. Four runs were conducted without altering the sail trim, simply changing items such as halyard, checkstay and shroud tension. The wind tunnel model has a solid wooden mast of the correct cross-sectional shape which means that, to achieve realistic bend and sag values at full scale equivalent, the torsional stiffness of the section was too high and consequently the values of twist are slightly lower than expected.

In the plots below, "run 24" was taken as the base case, which had generally insufficient forestay tension and luff tension on the mainsail. The tests were carried out at 25º AWA near the point of optimum C_L/C_D. Figure 17 shows the rig twist variation with height. By increasing the mainsail luff tension and bringing the checkstays on, the mast tube is brought straighter in the longitudinal axis (bend) and therefore tends to twist more. The resulting C_L/C_D values are given in Table 1. The trim changes listed are the changes applied to the immediately preceding run.

Table 1 - Values of C_L/C_D for different rig tunes

|	C_L/C_D	Progressive trim changes
Run 24 (base)	4.78	(base case)
Run 25	4.92	More jib and main luff tension, more checkstay tension
Run 26	4.58	Mast checkstay eased
Run 27	4.84	Mast backstay eased

Figure 18 shows the mast sag offset variation with height. This is worked out for each point as the transverse perpendicular distance away from an imaginary line joining the mast butt and the hounds and extending upwards. A negative value means that the mast is bending to windward of this straight line, even though the overall position is to leeward of the deck plane normal. This figure indicates that the S4 spreaders would need to be dropped down slightly by easing the diagonal below them to make a fair mast curve.

Figure 19 shows the luff bend and is calculated as the longitudinal distance to a line joining the mast tip and the top of the boom. Both the sag offset and luff bend are calculated from the global rig bend and sag, which are not presented here but are the main outputs from V-SPARS. They are in a way interrelated – "run 25" has the most luff tension and checkstay tension applied, hence the least luff curve and largest transverse deflection as shown by the sag offset. For interest Figure 19 also shows the value of the maximum luff curve deflection as a percentage of the mainsail luff length. The values are slightly lower than would be expected at full scale
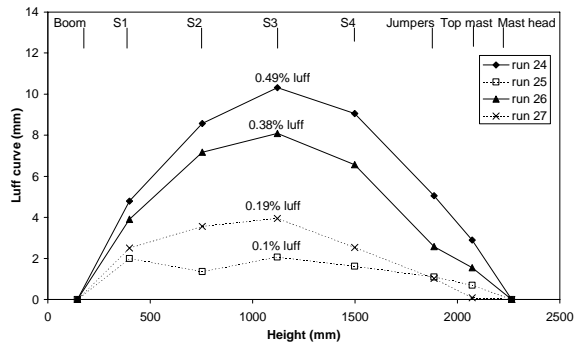
(approx 1%) as the model rig stiffness limited the amount of bend that could be achieved without rigging an inner forestay to pull forwards.
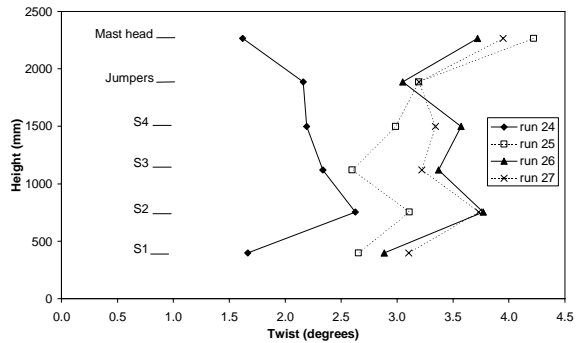
Figure 17 - Rig twist variation with different rig tunes
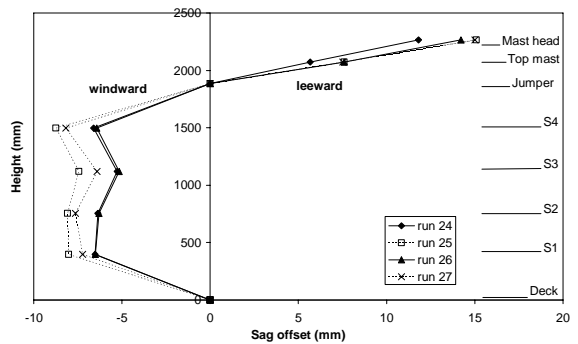
Figure 18. Sag offset between deck and hounds for different rig tunes

Figure 19. Luff curve between mast head and boom for different rig tunes

As V-SPARS combines the sail stripe data with the rig position in real time, it is possible to see in Figure 20 the following comparison of different rig setups. The output point cloud has been plotted using Rhino3D. The sail trim was not altered between runs. The tighter mainsail luff in run 25 brings the draft position forwards and tightens the leech, reducing the twist in the head. The jib forestay sag is reduced and the sail becomes flatter.

Figure 20. Rig and sail deflection with changing rig tune

4.3. Downwind testing

A set of simple downwind tests was carried out in order to determine the performance difference between two similar fractional A5 designs: the A5-1 at $1.02m^2$ and the A5-3 at $0.92m^2$ at 1:17 scale. One camera was positioned at the end of the bowsprit beneath the tack of the A5 and the mainsail camera was at ½ beam off the centerline and just aft of the spreaders . The wind tunnel driving force is plotted against apparent wind angle in Figure 21. This shows that the A5-1, which is the larger, flatter sail, performs better at the tighter angles and the A5-3 performs better at the deeper angle. The reason for the poor performance of the bigger sail, where a larger than normal region of separated flow was observed, is probably the omission of a suitable twist profile and vertical velocity gradient in the wind tunnel for these tests.
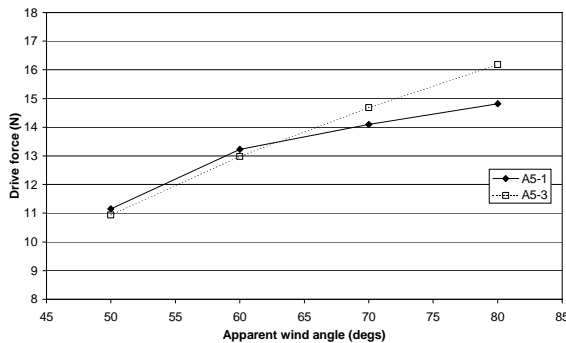

Figure 21. Model scale driving force against apparent wind angle for the A5-1 and A5-3

Figure 22 shows the two A5 sail shapes at 60º AWA. The surfaces have been created during post-processing from vertical curves passing through the stripes. The head location of the A5 is known, allowing the surface to be extended correctly to the head of the sail. The mainsail boom and head position have been extrapolated from the surface joining the measured stripes and have been given

no depth. The section of the A5 beneath the bottom stripe is unknown and cannot reliably be extrapolated. A wide-angle lens will allow a lower stripe to be measured, and maybe even the clew position itself. In this plot we can clearly see the flatter shape of the A5-1 (wireframe) which performs better at this angle compared with the A5-3 (surface).
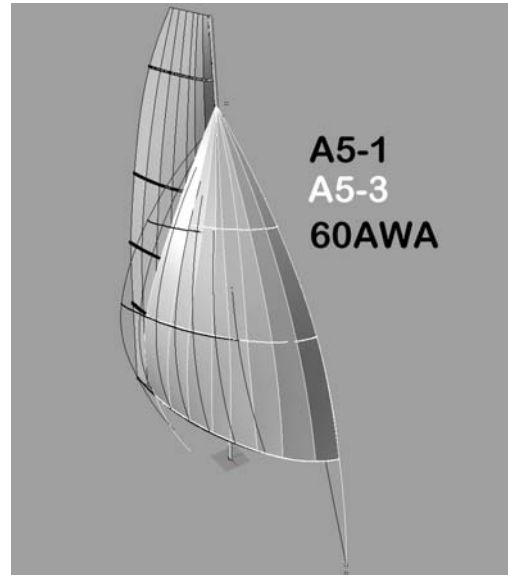

Figure 22. Comparison of downwind flying shapes at 60º AWA

Figure 23 and Figure 24 show the two A5 sails at 80º AWA. The relatively sharp bend in the middle stripe of the A5-1 can be seen and this may be causing the separation and hence worse performance at this angle. This would be less likely to occur if the sail were to be tested using the correct twist and velocity gradients.
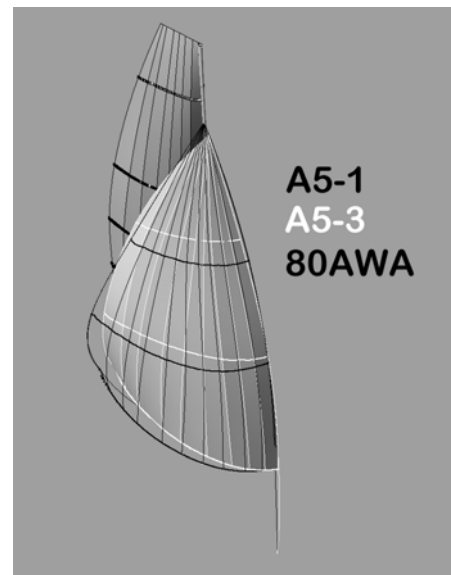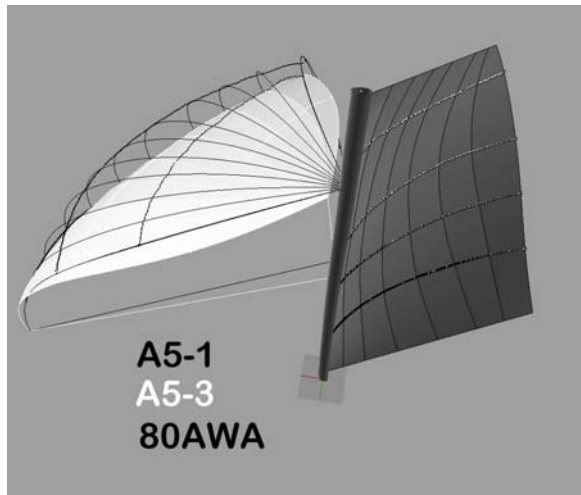

Figure 23. Comparison of downwind flying shapes at 80º AWA

Figure 24. Comparison of downwind flying shapes at 80° AWA

5. CONCLUSIONS

This paper has presented a method for assessing the sail shape of a number of sails in real time and combining them with the rig deflection. Validation tests in the wind tunnel have shown the perspective-correction algorithm to be robust and reasonably accurate. Examples of the system's capabilities have been given through upwind testing, rig tuning and downwind testing in the wind tunnel. Future work will include full-scale trials using wide angle lenses to be able to capture more of the sail shape.

References

1. "SailVision" (2008), *BSG Developments*, www.bsgdev.com

2. Olsson, O.J., Power, W.P., Bowman C.C., Palmer, T.G. & Clist, R.S. (1992), "SailSpy: a vision system for yacht sail shape measurement", *Proceedings of SPIE*, Vol. 1823, pp.256-261.

3. Masuyama, Y., Tahara, Y., Fukasawa, T. & Maeda, N. (2007), "Database of Sail Shapes vs. Sail Performance and Validation of Numerical Calculation for Upwind Condition" *18th Chesapeake Sailing Yacht Symposium*, SNAME, 11-31.

4. Krebber, B. & Hochkirch, K. (2006), "Numerical investigation on the effects of trim for a yacht rig", *Proceedings of the 2ⁿᵈ High Performance Yacht Design Conference*, RINA, 13-21.

5. Lindbom, P. (2006), "Laser scanning of sails and shape fitting to scan data", *Masters Thesis,* Yacht Research Unit, University of Auckland.

6. Fossati, F., Muggiasca, S., Viola, I.M. & Zasso, A. (2006), "Wind tunnel techniques for investigation and optimization of sailing yacht aerodynamics", *Proceedings of the 2ⁿᵈ High Performance Yacht Design Conference*, RINA, 105-113.

7. Yacht Research Unit Kiel (2008), http://www.yru-kiel.de/twistflowwindtunnel.html

8. École Polytechnique Fédérale de Lausanne (2007), http://alinghi.epfl.ch/page10241-en.html

9. Zhang, Z. (1998), "A flexible new technique for camera calibration", *Technical Report,* Microsoft Corporation, USA.

10. Flay, R.G.J. & Vuletich, I.J., (1995), "Development of a wind tunnel test facility for yacht aerodynamic studies", *Journal of Wind Engineering*, 231-258

11. Richards, P., Le Pelley, D., Cazala, A. McCarty, M., Hansen, H. & Moore, W., (2006), "The use of independent supports and semi-rigid sails in wind tunnel studies" , *Proceeding s of the 2ⁿᵈ High Performance Yacht Design Conference*, RINA, 114-122.

12. Hansen, H., Richards, P.J., & Jackson, P.S., (2006), "Enhanced wind tunnel and full scale force comparison", *18ᵗʰ Chesapeake Sailing Symposium*, SNAME.

13. Hansen, H., Jackson, P.S. & Hochkirch, K. (2003) "Real time Velocity Prediction Program for wind tunnel testing of Sailing Yachts", *Proceedings of The Modern Yacht Conference,* RINA.